Journal of Power Sources 195 (2010) 7818–7824

Contents lists available at ScienceDirect

Journal of Power Sources

journal homepage: www.elsevier.com/locate/jpowsour

Cell temperature measurements in micro-tubular, single-chamber, solid oxide fuel cells (MT–SC–SOFCs)

N. Akhtar[a,b,*], S.P. Decent[a], K. Kendall[b]

[a] School of Applied Mathematics, University of Birmingham, B15 2TT, UK
[b] Department of Chemical Engineering, University of Birmingham, B15 2TT, UK

ARTICLE INFO

Article history:
Received 4 April 2009
Received in revised form 21 April 2009
Accepted 28 April 2009
Available online 18 May 2009

Keywords:
Solid oxide fuel cell
Single-chamber
Air–fuel mixture
Temperature
Micro-tubular

ABSTRACT

Anode supported, micro-tubular, solid oxide fuel cells made of nickel, yttria-stabilized zirconia (Ni–YSZ) anode, yttria-stabilized zirconia (YSZ) electrolyte and lanthanum strontium manganite (LSM) cathode have been prepared and operated under single-chamber conditions. Four different cells with varying cathode location/size, i.e. inlet, center, outlet and full size have been compared. The highest temperature rise of ~93 °C and the highest power density of ~36 mW cm^{-2} (at a furnace temperature of 750 °C with methane/air = 25/60 mL min^{-1}) was observed in the case of cathode-inlet configuration. The scanning electron microscope (SEM) analysis shows that both the anode and cathode were badly damaged near the cell inlet in case of cathode-inlet configuration. On the contrary, both of the electrodes remained undamaged in case of cathode-outlet configuration.

1. Introduction

The conventional solid oxide fuel cells provide greater flexibility in terms of fuel to be supplied to the anode side. They can be run on variety of fuels including hydrogen, natural gas, biogas, diesel, methanol, ethanol, etc. [1]. However, most of these fuels (other than the hydrogen) have to be converted into hydrogen (and in some cases to carbon monoxide) either internally or externally [2]. Internal fuel processing (directly in the stack) is preferred over external (in a separate catalytic reactor) one, because it can simplify the overall design leading to higher overall efficiencies [3]. The different approaches generally adopted for fuel processing are steam reforming, dry reforming, partial oxidation and autothermal reforming as given below [4]:

(1) Steam reforming:

$$CH_4 + H_2O \rightarrow CO + 3H_2, \qquad \Delta H = +206\,\text{kJ mol}^{-1} \tag{1}$$

(2) Dry reforming:

$$CH_4 + CO_2 \rightarrow 2CO + 2H_2, \qquad \Delta H = +247\,\text{kJ mol}^{-1} \tag{2}$$

(3) Partial oxidation:

$$CH_4 + 0.5O_2 \rightarrow CO + 2H_2, \qquad \Delta H = -36\,\text{kJ mol}^{-1} \tag{3}$$

(4) Autothermal reforming:

$$CH_4 + 0.5O_2 + H_2O \rightarrow CO_2 + 3H_2, \qquad \Delta H = -77\,\text{kJ mol}^{-1} \tag{4}$$

The most widely adopted reforming process is the steam (wet) reforming, whereas the other, namely, the dry (using carbon dioxide) reforming is less attractive as it gives less hydrogen yields compared with steam reforming reaction (see Eqs. (1) and (2)). One common thing in both of these reforming methods is their endothermic nature, i.e. requiring heat for reaction to proceed. The state of the art SOFC nickel/yttria-stabilized zirconia anodes are found to be active towards steam reforming reaction; the carbon deposition is of a major concern in nickel-based anodes [5–7]. The high steam-to-carbon ratio is typically required to suppress carbon formation, which can lower the electrical efficiency due to fuel dilution [2]. The other problem associated with the reforming reaction is the strong cooling effect that can generate large thermal gradients across the cell. It has been observed that this endothermic reaction is very strong near the cell entrance [2].

The other less employed fuel processing technique is the partial oxidation (Eq. (3)), which can circumvent the problem of anode coking (to a certain extent) in cases where nickel is used as the catalyst [8]. Moreover, if pure oxygen (rather than air) is used for the par-

* Corresponding author at: School of Applied Mathematics, University of Birmingham, Edgbaston, Birmingham B15 2TT, UK. Tel.: +44 7726 126748; fax: +44 121 4143389.
E-mail address: nxa675@bham.ac.uk (N. Akhtar).

0378-7753/$ – see front matter © 2009 Elsevier B.V. All rights reserved.
doi:10.1016/j.jpowsour.2009.04.078

tial oxidation then the fuel dilution problem can also be overcome [4]. Though, it is generally believed that the partial oxidation offers certain advantages (as mentioned above) over steam reforming, the exothermic extent of partial oxidation in nickel-based conventional SOFCs is less addressed [3,9]. Yet, there are few experimental reports on partial oxidation using nickel anodes in SC–SOFCs stating similar problems of large thermal gradients as in the case of steam reforming [10–15]. However, the nature of these thermal gradients is exothermic (rather than endothermic as was in steam reforming) and can be even worse than the gradients produced during steam reforming reaction.

In order to tackle the problem arising due to thermal gradients developed in both of the above cases, the partial oxidation can operate in conjunction with steam reforming via a route referred to as autothermal reforming. This reaction is mildly exothermic, can harmonize thermal gradients and improve hydrogen yield (Eq. (4)). In addition, autothermal reforming is less susceptible to carbon formation as compared to steam reforming because of the presence of both the steam and oxygen directly at the anode [9].

Besides autothermal reforming is an attractive technique, it is less used in practice possibly due to very complex anode chemistry and because of strict control of steam-to-carbon and fuel-to-oxygen ratios under long term operation [16]. Not only in conventional SOFCs, the use of autothermal reforming in single-chamber solid oxide fuel cells (SC–SOFCs) could help minimize temperature gradients over the cell length. However, to the authors knowledge there is no such study employing autothermal reforming in SC–SOFCs, only Ahn et al. used a slightly wet methane (3% steam) in their study on co-planar type SC–SOFCs [17]. Most of the studies reported on SC–SOFCs are based on partial oxidation reaction with a very little discussion on thermal counter effects [10,13]. As said earlier, the partial oxidation is an exothermic reaction that can produce severe thermal gradients. These gradients can develop thermal strains, crack production, propagation, thereby resulting in a premature failure of the cell. Not only this, these thermal gradients could be even more severe if occur in the form of a thermal shock. It is therefore very necessary to study their contribution in affecting the cell's long-term stability via thermally driven degradation mechanism. This background led us to investigate the effect of partial oxidation on thermal gradients in SC–SOFCs.

Single-chamber solid oxide fuel cell's operation depends upon catalytic activity of the anode and electro-catalytic activity of the cathode [12]. Moreover, the high selectivity of both electrodes towards electrochemical reaction (i.e. fuel oxidation in the anode and oxygen reduction in the cathode) is essential for better performance [14,15]. The catalytic activity of the electrode materials (particularly of the anode) generates large amounts of heat, which defines the actual cell temperature that differs significantly from the furnace temperature [10,12,13]. The amount of heat release depends upon many parameters such as the type of fuel, fuel-to-oxygen ratio, flow rate, electrode materials, active area, cathode-to-anode area ratio and the electrode placement [18]. While it is generally believed that the core reaction in the anode (of an SC–SOFC) is a partial oxidation reaction, recently Hao et al. [19] suggested three different reaction zones in the SC–SOFC anode. According to them, there exists a thin outer layer in which oxygen is nearly fully consumed in oxidizing methane and hydrogen, followed by a reforming region, and then a water gas shift region deep within the anode. The existence of a complete combustion reaction is more severe than the partial oxidation and can generate large amounts of exothermic heat depending upon the type of fuel employed. Such overheating on one side might be advantageous, as one can make use of this heat to thermally self-sustain the system [20]. On the other hand, this can result in structural damage and thermally driven degradation problems as will be described later in this study.

In this study, we made an attempt to investigate the local temperature distribution across the cell length with varying active area. For this purpose four different cells with varying cathode location/size, i.e. inlet, center, outlet and full size have been prepared and tested. In the following discussion, all the results are normalized against the corresponding geometric cathode areas. Finally, scanning electron microscopy (SEM) analysis has been performed in order to observe changes in the cell structure.

2. Experimental

Four different cell configurations have been prepared as shown in Fig. 1. The cells consist of Ni–YSZ/YSZ/LSM, anode/electrolyte/cathode assembly (Fig. 2). The geometry dimensions and cell preparation methodology has been described in our earlier publication [21]. The cell was kept in the center of the gas-chamber tube with a holder. A brick furnace was controlled by a Eurotherm™

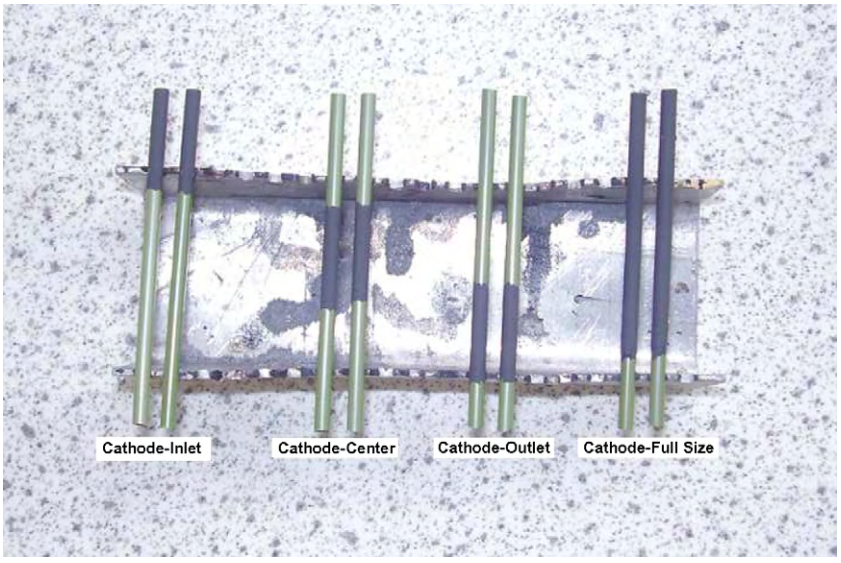

Fig. 1. Four different cells with varying cathode location/size.

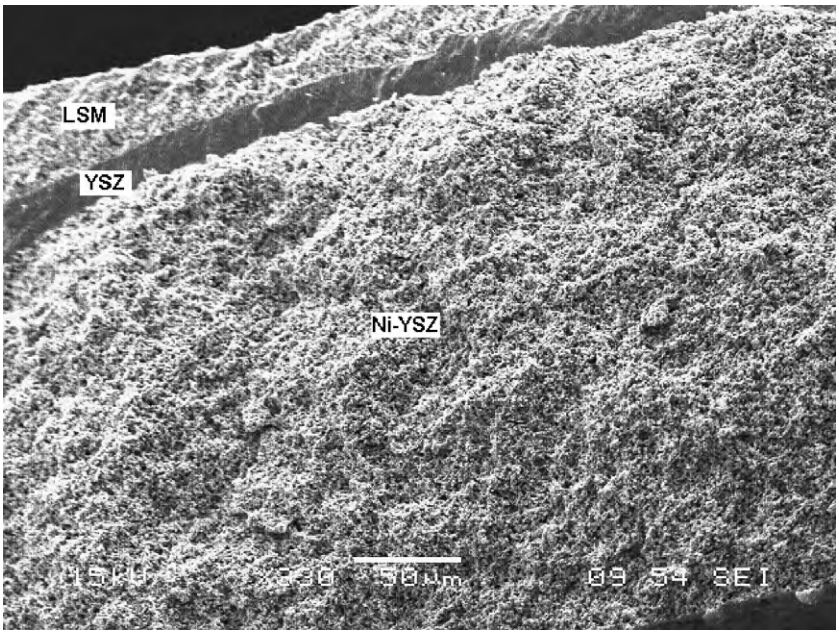

Fig. 2. SEM photograph of anode–electrolyte–cathode cross-section.

2402 controller with a K-type thermocouple to measure the furnace temperature. An additional thermocouple was inserted into the micro-tube to measure the anode surface temperature as shown in Fig. 3. Since the chemical reaction is taking place at the anode (via partial or full oxidation of the methane), it was necessary to measure the temperature directly at the anode surface because of large amount of heat generated at this location. The rest of the geometrical setup was the same as reported earlier in Ref. [21].

The anode surface temperature was measured at three different locations along the length, i.e. near the inlet (3 mm from inlet), at the center (18 mm from inlet) and near the cell outlet (36 mm from inlet). The active cell length was 18 mm for the cathode-inlet, center and outlet configurations whereas for the cathode full-size configuration, it was 39 mm with a total length of 55 mm for all cells. All cells were supplied with methane/air mixture of 25/60 mL min^{-1}. The furnace temperature (T_F) was varied from 550 to 800 °C and the cell temperature was measured for all four configurations (as described above).

3. Results and discussion

3.1. Cell temperature

In Fig. 4(a–f), cell temperature (at various furnace temperatures of 550–800 °C) is shown for inlet, center, outlet and full-size configurations. At low temperature such as 550 and 600 °C, the highest temperature rise (at the middle of the cell) is observed in cathode-center configuration (Fig. 4(a) and (b)).

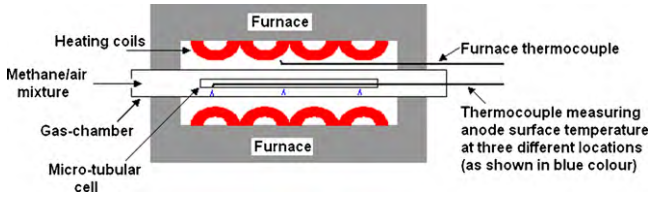

Fig. 3. Temperature measurement setup.

However, contrary to this as we move along increasing furnace temperatures, the highest cell temperature is observed near the cell inlet in case of cathode-full size and cathode-inlet configurations (Fig. 4(c–f)). Clearly the highest temperature rise in case of cathode-full size is misleading, since it has larger active area ($A = 2.45\ cm^2$) as compared to the other three configurations ($A = 1.13\ cm^2$). The area-normalized values of temperature show that with increasing furnace temperature, cathode-inlet configuration has the highest temperature. Furthermore, the local cell temperature is pronounced near the cell inlet for this configuration. This observation is further supported by the following arguments:

- The nickel anode seems to be active towards fresh air/fuel mixture. As we move along the cell length, the mixing ratio may vary due to catalytic and electrochemical reactions. It appears that the reaction behaviour of nickel is very similar to that observed in case of steam reforming (i.e. the cooling effect near the cell inlet due to endothermic reaction). In this case, it is heating effect near the cell inlet due to exothermic reaction.
- The cathode loses its selectivity towards electrochemical oxidation (or becomes catalytically active towards methane oxidation) as the temperature increases. The presence of cathode at the inlet is an addition of parasitic loss (or in other words heat addition) at that location.
- The commonly used nickel anode is not perfectly selective for partial oxidation reaction and loses its selectivity as the temperature increases. As pointed out by Hao et al. [19], the oxygen could be nearly fully consumed in the outermost anode region (near the anode–gas interface) via complete combustion mechanism. It is obvious from this argument that the increase in temperature will promote full combustion instead of partial oxidation, thereby further addition of heat.

It is important to note that we did not measure the cell temperature for full-size configuration at $T_F = 800$ °C, because of similar expected temperature rise may reach close to the melting point of silver and could damage the current collecting wires. Further to this, important information coming out from cathode-center

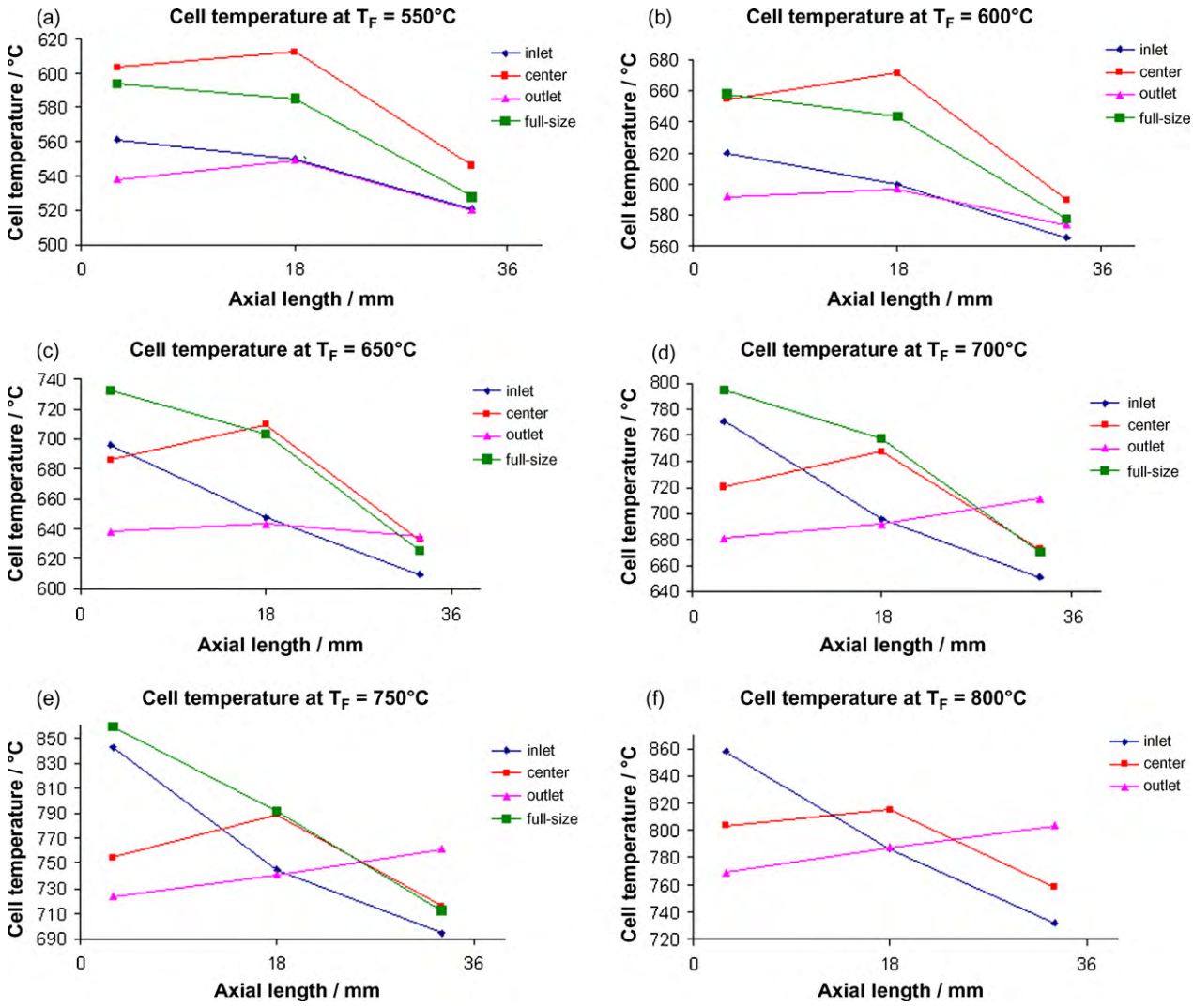

Fig. 4. Anode surface temperatures at (a) 550 °C, (b) 600 °C, (c) 650 °C, (d) 700 °C, (e) 750 °C, (f) 800 °C furnace temperatures (methane/air = 25/60 mL min^{-1}).

and outlet configurations (pink and red curves in Fig. 4(d–f)) is that it is not only the nickel anode, which is solely responsible for highest temperature rise in case of cathode inlet, the presence of cathode has a greater influence. For example, the cathode-center and cathode-outlet configurations show a clear maximum temperature rise near the center and outlet of the cell, respectively. This effect was not that marginal at low furnace temperatures (550–600 °C) suggesting that the cathode activity towards methane oxidation at higher temperature could be the reason. Moreover, the highest cell temperature in cathode-center configuration suggests that the center location is acting as a heat confinement and this effect is dominant at low temperatures (550–600 °C). At furnace temperatures greater than 600 °C, the heat contribution due to catalytic/electrochemical oxidation of fresh air/fuel mixture is becoming dominant.

3.2. Open circuit voltage (OCV)

The effect of furnace heating on the open circuit voltage for four different configurations is shown in Fig. 5. As can be seen the highest OCV is observed in case of cathode-outlet configuration. This observation is in good agreement with the study done by Morel et al. [10]. They used closed gas distribution plates (GDP) to prevent any gas leakage due to combustion resulting in volume expansion. Their idea was to maintain high oxygen partial pressures on the cathode side by confining the surrounding fresh gas mixture in cathode-outlet configuration. Our study further confirms their hypothesis of local gas confinement resulting in higher OCV in cathode-outlet configuration. The micro-tubular geometry is itself acting as a closed GDP and preventing any cross-diffusion across the electrodes. The cathode-outlet configuration further confirms the availability of fresh air/fuel mixture with nearly unaltered oxygen

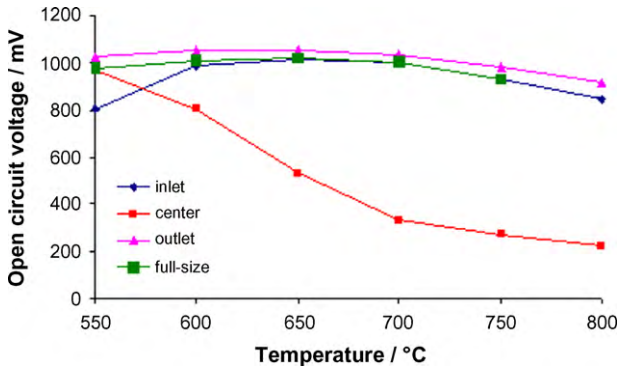

Fig. 5. Temperature vs. open circuit voltage (methane/air = 25/60 mL min^{-1}).

partial pressure at the cathode located near the cell outlet. Contrary to this the air/fuel mixture in the anode (located inside of the micro-tube) is continuously depleted and becomes oxygen deficient when it reaches to the cell outlet. The higher oxygen partial pressure differential across the electrodes gives a clear indication of highest OCV in cathode-outlet configuration.

The cathode-center configuration was giving very low OCV as we increase furnace temperature. This can be explained by two mechanisms: (1) as previously mentioned the cathode parasitic losses (due to fuel oxidation) increase with increasing temperature, (2) the gas velocity (and the amount of gas available) in the vicinity of the center of the tube could be limited which can increase the residence time for parasitic reactions at the cathode located at the center.

3.3. Output performance

For measuring the output performance, the cells were supplied with a methane/air mixture of 25/60 mL min^{-1} for all four configurations. The flow rate was kept very low in order to improve the effective fuel utilization and electrical efficiency. The highest effective fuel utilization and electrical efficiency was 2.35% and 1.13% (at a furnace temperature of 750 °C) for cathode-full size, respectively (for details about this calculation the reader should refer to Ref. [21]). The other three configurations (i.e. cathode-inlet, center and outlet) showed even lower fuel utilization because of less amount of total current generated due to less active area.

Fig. 6 shows the performance curves for four configurations. As can be seen at low temperature (less than 600 °C) cathode-center configuration is giving the best performance (Fig. 6(a)). However, as the temperature increases beyond 600 °C, its performance is becoming worse than the other three configurations (see Fig. 6(b–e)). This trend is due to steep decrease in OCV of the cathode-center position as discussed above. It should be noted that the OCV provides the driving force for current flow once the circuit is opened.

All other configurations (i.e. inlet, outlet and full-size) follow nearly same trend with increase in temperature, i.e. the electrolyte conductivity improves with increasing temperature, and therefore more current is expected. The best performance was observed in case of cathode-inlet configuration in the temperature range of 700–750 °C, which is the most practical operating regime for high temperature ionic conductor (YSZ) employed in SC–SOFCs. The highest cell temperature in the cathode-inlet configuration enhances local ionic conductivity resulting in improved performance. Furthermore, it is also observed that with increas-

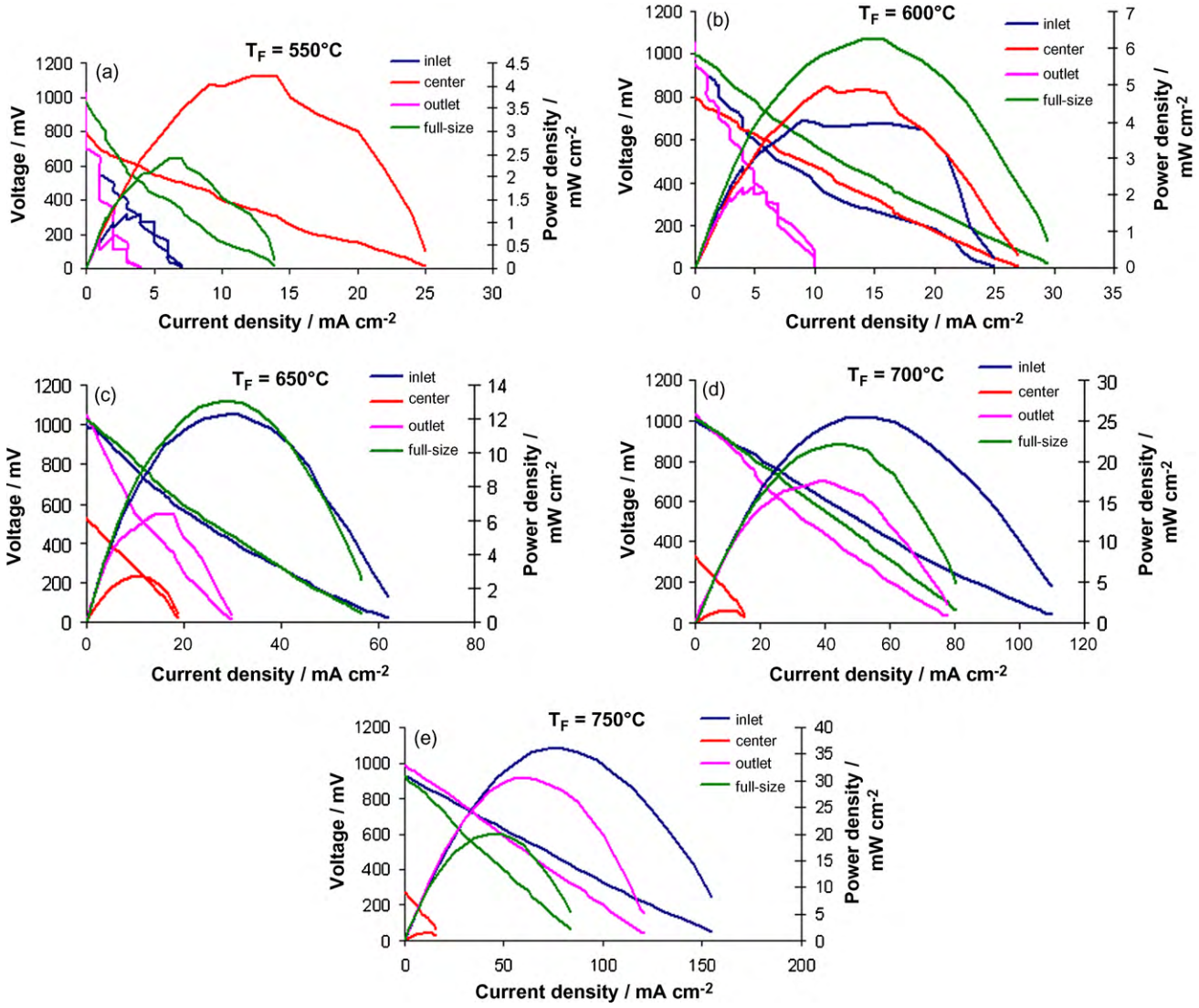

Fig. 6. Performance curves at (a) 550 °C, (b) 600 °C, (c) 650 °C, (d) 700 °C, (e) 750 °C furnace temperatures (methane/air = 25/60 mL min^{-1}).

ing temperature cathode-outlet configuration is showing improved performance. The next highest performance at 750 °C is of cathode-outlet configuration (Fig. 6(e)). It is suggested that in this case the inner anode is acting as a catalytic reactor up to two-third of the cell length, thus supplying pre-reformed reactants (such as hydrogen and carbon monoxide) to the last part of cell where the cathode is located and to be ready for electrochemical reactions.

3.4. Structural analysis using scanning electron microscopy

The above results show that the cathode inlet configuration has the highest temperature rise and the cathode-outlet configuration is undergoing less temperature gradient across the length. We therefore analyzed these cells by taking a sample of anode and cathode surfaces near the inlet for both configurations. The SEM photograph (Fig. 7(a and b)) shows that both the anode and cathode surfaces (near the inlet) are badly damaged and cracked in case of cathode-inlet configuration. This effect confirms the severity of local temperature rise near the inlet. On the contrary, Fig. 8(a and b) shows that both the anode and cathode surfaces (near the inlet) were relatively undamaged and no visible crack was observed in case of cathode-outlet configuration.

It is therefore concluded that the local temperature may have a serious effect in structural damage that could lead into thermal shock problems.

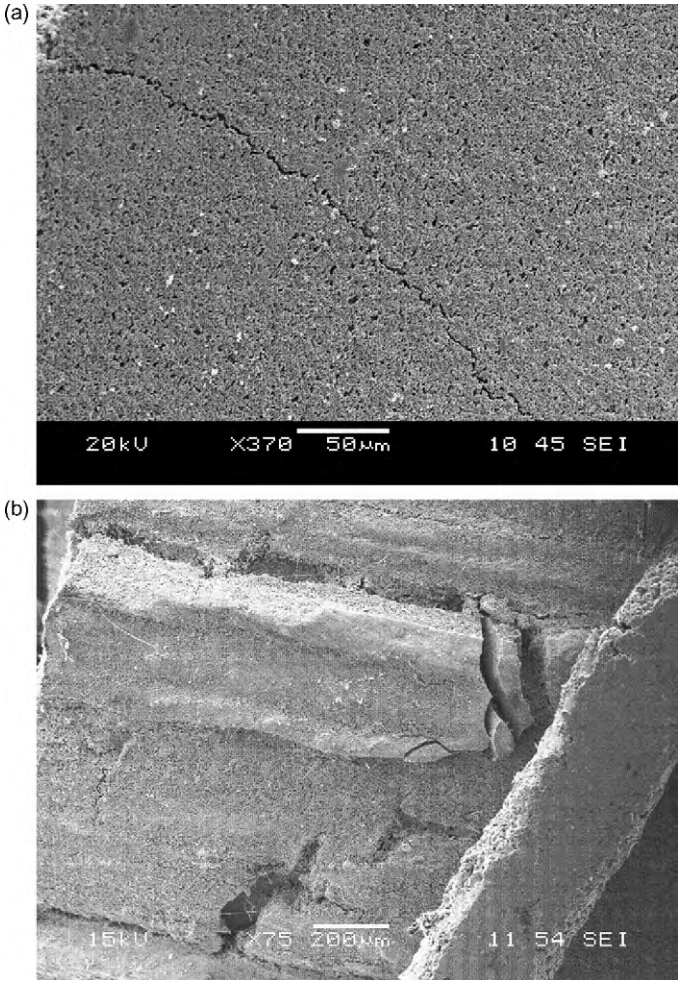

Fig. 7. Cracked anode (a) and damaged cathode (b) near the cell inlet for cathode-inlet configuration.

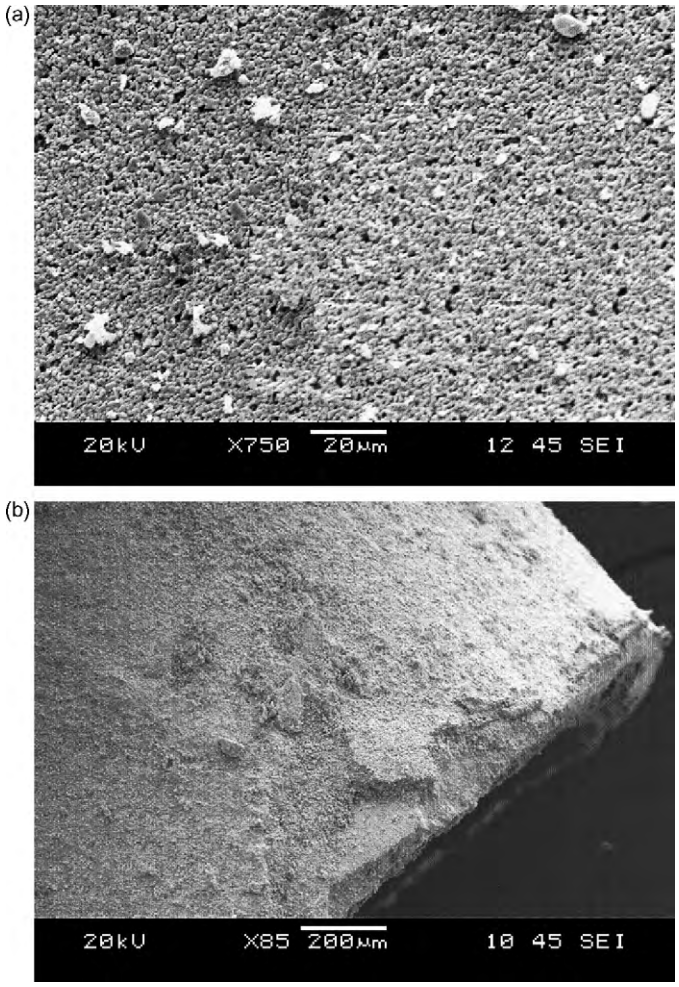

Fig. 8. Undamaged anode (a) and cathode (b) near the cell inlet for cathode-outlet configuration.

4. Conclusions

The study shows that the highest temperature rise of ~93 °C (at a furnace temperature of 750 °C with methane/air = 25/60 mL min^{-1}) is observed in case of cathode-inlet configuration. It is also observed that the cell inlet is more sensitive to damage because of large exothermic heat due to fuel oxidation directly at the anode inlet. The cathode-outlet configuration shows little temperature gradients as compared to all other configurations. This design may be preferred because of less thermal stresses. Since the silver current collecting wire used in this study has a fairly low melting point (960 °C), it is quite possible that the generated heat may accumulate, raise the local temperature and finally break the silver wire. In this case, either the replacement of current collecting wire must be sought or the operating temperature must be kept well below the silver melting point. The operation at low temperature does not seem feasible because the ionic conductivity of YSZ electrolyte sharply drops with decrease in temperature.

The present study demonstrates that the continuous heat generation can result in local hot spots and structural damage at the cell inlet. Not only this, the inhomogeneous temperature distributions and steep temperature gradients along the length of the fuel cell can give rise to state of compression and tension. The power density is also highly non-uniform over the cell length because of large variations in the ionic conductivity of the electrolyte. While it is generally believed that this exothermic heat is useful in order to lower the external heat demand, its negative effects have been

simply neglected. However, it should be noted that its possible contribution to the early degradation and structural damage of SC–SOFCs cannot be compromised, especially with the use of higher hydrocarbon fuels that produce even larger quantities of reaction heat.

Acknowledgments

The authors would like to thank E.ON-UK and EPSRC-UK for funding Mr. Naveed Akhtar through Dorothy Hodgkin Postgraduate Award (DHPA) scheme.

References

[1] S.C. Singhal, K. Kendall, High Temperature Solid Oxide Fuel Cells: Fundamentals, Design and Applications, Elsevier, Kidlington Oxford, 2003, p. 19.
[2] P. Aguiar, C.S. Adjiman, N.P. Brandon, J. Power Sources 138 (2004) 120–136.
[3] P.K. Cheekatamarla, C.M. Finnerty, Y. Du, J. Jiang, J. Dong, P.G. Dewald, C.R. Robinson, J. Power Sources 188 (2009) 521–526.
[4] Y.-C. Yang, B.-J. Lee, Y.-N. Chun, Energy 34 (2009) 172–177.
[5] S. Yoon, J. Bae, S. Kim, Y.-S. Yoo, J. Power Sources 192 (2009) 360–366.
[6] Y. Wang, W. Wang, X. Hong, Y. Li, Z. Zhang, Int. J. Hydrogen Energy 34 (2009) 2252–2259.
[7] F. Pompeo, D. Gazzoli, N.N. Nichio, Int. J. Hydrogen Energy 34 (2009) 2260–2268.
[8] P. Piroonlerkgul, S. Assabumrungrat, N. Laosiripojana, A.A. Adesina, Chem. Eng. J. 140 (2008) 341–351.
[9] S. Ahmed, M. Krumpelt, Int. J. Hydrogen Energy 26 (2001) 291–301.
[10] B. Morel, R. Roberge, S. Savoie, T.W. Napporn, M. Meunier, J. Power Sources 186 (2009) 89–95.
[11] Z. Shao, C. Kwak, S.M. Haile, Solid State Ionics 175 (2004) 39–46.
[12] T. Hibino, A. Hashimoto, T. Inoue, J. Tokuno, S. Yoshida, M. Sano, J. Electrochem. Soc. 148 (2001) A544–A549.
[13] T.W. Napporn, F. Morin, M. Meunier, Electrochem. Solid-State Lett. 7 (2004) A60–A62.
[14] T. Suzuki, P. Jasinski, V. Petrovsky, H.U. Anderson, F. Dogan, J. Electrochem. Soc. 151 (2004) A1473–A1476.
[15] Z. Shao, J. Mederos, W.C. Chueh, S.M. Haile, J. Power Sources 162 (2006) 589–596.
[16] M.Z. Nezhad, S. Rowshanzamir, M.H. Eikani, Int. J. Hydrogen Energy 34 (2009) 1292–1300.
[17] S.-J. Ahn, Y.-B. Kim, J. Moon, J.-H. Lee, J. Kim, J. Power Sources 171 (2007) 511–516.
[18] X.J. Bedard, T.W. Napporn, R. Roberge, M. Meunier, J. Electrochem. Soc. 154 (2007) B305–B309.
[19] Y. Hao, D.G. Goodwin, J. Electrochem. Soc. 155 (2008) B666–B674.
[20] Z. Shao, S.M. Haile, J. Ahn, P.D. Ronney, Z. Zhan, S.A. Barnett, Nature 435 (2005) 795–798.
[21] N. Akhtar, S.P. Decent, D. Loghin, K. Kendall, J. Power Sources, doi:10.1016/j.jpowsour.2009.01.032.